ORIGINAL ARTICLE

Tran Huu Nam ⃝ · **I. Petríková** · **B. Marvalová**

Stress relaxation behavior of isotropic and anisotropic magnetorheological elastomers

Abstract The paper presents an experimental study and numerical simulation of stress relaxation behavior of isotropic and anisotropic magnetorheological elastomers (MREs) made from silicone rubber filled with micro-sized carbonyl iron powder. Effects of applied constant strains and magnetic fields of an electromagnet on the stress relaxation of the MREs were investigated for 10 h using the single relaxation test with double-lap shear samples. The isotropic MRE showed a linearly elastic behavior, while the anisotropic MRE indicated a highly nonlinear elastic response. The shear stress and relaxation modulus of anisotropic MRE are much higher than those of isotropic MRE. The shear stress of the MREs increased with increasing the constant strain, while their relaxation modulus decreased. The shear stress and relaxation modulus of the MREs within the first 0.25 h boosted with raising the magnetic flux density to about 0.5 T. However, the shear stress and relaxation modulus of the MREs under strong magnetic fields declined considerably after 0.25 h testing. This reduction was attributed to the temperature rise in the MRE samples caused by the heating of the electromagnet. The stress relaxation behavior of the MREs was examined using a four-parameter fractional derivative model. The model parameters were obtained by fitting the relaxation modulus to the measured data of the MREs. The shear stress and relaxation modulus with long-term predictions estimated from the studied model were in good agreement with the measured data for the MREs at various applied strains and under low magnetic fields. The model-predicted values did not agree well with the experimental data of the MREs under high magnetic fields because of the sample temperature gain caused by heat generation of the electromagnet. Therefore, the investigated model can be used to predict the long-term relaxation stress of the MREs under high magnetic fields of permanent magnets.

Keywords Magnetorheological elastomer · Stress relaxation behavior · Fractional derivative model · Magnetic field · Electromagnet · Relaxation test

1 Introduction

Magnetorheological elastomers (MREs) were introduced in 1983 by Rigbi and Jilken [1]. As a type of smart elastomeric composite materials, MREs have been greatly interested in recent years because of their change in the mechanical and rheological properties under the application of an external magnetic field [2–5]. Besides, MREs can change in their shape in response to magnetic fields. Therefore, they are currently explored as programmable shape-morphing materials [6,7]. The change in the MRE properties is known as the magnetorheological (MR) effect. MREs exhibit the controllable stiffness and damping properties as well as trans-

Communicated by Andreas Öchsner.

T. H. Nam (✉) · I. Petríková · B. Marvalová
Department of Applied Mechanics, Faculty of Mechanical Engineering, Technical University of Liberec, Studentská 1402/2, 461 17 Liberec 1, Czech Republic
E-mail: nam.tran.huu@tul.cz; thnam.hut@gmail.com

forming their shapes in nearly real-time in response to applied magnetic fields. The controllable magnetic field-dependent stiffness, shape, and damping properties of MREs make them used in a variety of engineering applications, such as vibration absorbers [8–10], vibration isolators [11–13], sensors and actuators [14–16], peristaltic pump [17], engine mounts for automobile [18], metamaterials [19–21], adaptive stiffness devices [22], shape memory elastomer [23], shape-morphing structures [6,7], and even soft continuum robots [24,25]. Therefore, studies of the time-dependent mechanical properties of MREs in an external magnetic field under various loading conditions are essential for real engineering applications.

MREs have been produced by filling ferromagnetic particles into non-magnetic elastomeric matrices. The non-magnetic elastomers used for MREs include natural rubbers, silicone rubbers, vinyl rubbers, polyurethanes, thermosets, and thermoplastics [1–4,26–30]. Among these elastomers, silicone rubbers are the most widely used as matrix materials for the production of MREs. Silicone rubbers have extraordinary properties such as low viscosities and easy suspension of ferromagnetic particles that make them attractive in applications of MREs [3]. Besides, silicone rubbers are non-toxic, non-flammable, less temperature-sensitive, less dissipative, and highly deformable [4]. Ferromagnetic particles are field-sensitive components of MREs and are mainly responsible for the magnetic field-dependent properties [29]. Among the ferromagnetic particles, carbonyl iron powders (CIPs) are the most common type in manufacturing MREs because of their high magnetic permeability, high magnetic saturation, and low magnetic remnant [3,30]. The properties of MREs greatly depend on the distribution of CIPs [31]. The distribution of CIPs in MREs can be either random (isotropic) or partially aligned in chains by curing in the presence of a magnetic field (anisotropic) [3,31–33].

MREs are viscoelastic elastomeric composite materials, therefore they inherit predominant properties of the elastomeric matrix such as large deformations, stress softening effect, amplitude and frequency dependency, time- and temperature-dependent features. The time-dependent rheological properties of viscoelastic elastomeric materials have been examined using creep and stress relaxation tests [32–40]. However, research on the stress relaxation of elastomeric materials has been usually conducted in short-term periods. Nam et al. [32,33] investigated the shear stress relaxation of isotropic and anisotropic MREs for 1000 sec in the single-step relaxation test and 10 min of each step in the multi-step relaxation test. Amin et al. [34] studied the simple stress relaxation behavior of filled natural rubber in compression and shear regimes. The relaxation behavior was investigated for 10 min in the compression tests and 60 min in the shear tests. Besides, the simple tensile and compressive stress relaxations of filled rubber composites were examined for 20 min [35]. Recently, the shear stress relaxation behavior of MRE made of polyurethane and epoxy resin was studied within 1000 sec [38]. Most recently, Johari et al. [40] presented the shear band formation in MRE under stress relaxation for about 30 min.

Many studies showed that the stress relaxation behavior of viscoelastic elastomeric materials depends strongly on the temperature [38,41–45]. Qi et al. [38] investigated the effect of temperature on the stress relaxation response of MRE based on the polyurethane/epoxy interpenetrating polymer networks matrix and concluded that the relaxation shear stress reduces with increasing temperature and the stress relaxes more strongly as the temperature enhances. Rey et al. [41] examined the influence of temperature on the mechanical hysteresis, stress softening, and stress relaxation of filled and unfilled silicone rubbers. They also reported that the relaxation stress decreases with rising temperature. Moreover, the temperature-dependent thermo-mechanical behavior of a fluoro-elastomer was investigated through simple relaxation tests under tension and compression loading conditions and multi-step relaxation tests [42]. The research results indicated that the higher the temperature, the lower the stress relaxation. Besides, the effect of the temperature on the compressive stress relaxation is more pronounced than the tensile one. Recently, Wen et al. [45] studied temperature-dependent magneto-mechanical properties of MREs and reported that the relaxation modulus of MREs decreases with increasing temperature.

The viscoelastic mechanical properties of MREs can be studied numerically using constitutive models with fractional calculus [46–51]. Fractional calculus was proved to be a powerful tool to characterize the viscoelastic behaviors of materials [46]. Fractional derivative models based on classical viscoelastic models (Maxwell, Kelvin–Voigt, Zener, Poynting–Thomson, etc.) have been constructed by different combinations of elastic spring and fractional dashpot [47,48]. The elastic spring is used to describe the time-independent elastic behavior, while the fractional dashpot is applied to represent the dependence of viscous behavior on the deformation history. There have been several fractional derivatives applied for fractional viscoelastic models, such as the Riemann–Liouville derivative, the Caputo derivative, the Hadamard derivative, and fractional derivatives with exponential function or Mittag-Leffler function. The Mittag-Leffler function was considered as a general empirical law for both creep and relaxation functions [46]. The Mittag-Leffler function is appropriate

for fitting the experimental data of stress relaxation and allows for a straight prediction of the frequency-dependent complex modulus of polyurethane foams [51].

The study of time-dependent rheological properties of MREs in a magnetic field is crucial for real engineering applications. For this paper, isotropic and anisotropic MREs were fabricated from silicone rubber and micro-sized CIPs. The experimental study and numerical simulation of the stress relaxation behavior of the isotropic and anisotropic MREs were conducted. The stress relaxation response of the MREs was investigated for a mid-term period of 10 h using the single relaxation test with double-lap shear specimens. The effects of applied constant strains and magnetic fields of the electromagnet on the stress relaxation of the MREs were examined. Besides, the influences of the temperature rise in the MRE samples caused by potential magnetic fields on the stress relaxation of the MREs were investigated. The stress relaxation of the MREs was calculated using a four-parameter fractional derivative viscoelastic model with the Mittag-Leffler function. The fitting parameters of the model with the measured data were used to predict the long-term stress relaxation of the isotropic and anisotropic MREs. The dependence of shear stress and relaxation modulus of the MREs on the constant strain level and magnetic flux density (MFD) was numerically calculated using the studied model.

2 Experimental

2.1 Materials

The isotropic and anisotropic MREs are produced from micro-sized CIPs, RTV silicone rubber ZA13, and its catalyst. The micro-sized CIPs (type: 44890) supplied by Sigma-Aldrich (USA) have a purity of 99.5% and a density of 7.86 g/cm^3. The grain size of the CIPs is between 5 and 9 μ m. The RTV silicone rubber ZA13 and its catalyst are developed by Zhermack S.P.A (Italy) and are provided by Havel Composites Ltd. (Czech Republic). The microstructural morphology of the CIPs and their diameter as a function of the volume fraction in overall distribution can be found in our earlier papers [31–33].

2.2 Fabrication of isotropic and anisotropic MREs

The production of isotropic MRE is described as follows. Firstly, the RTV silicone rubber ZA13 was mixed with its catalyst in the mass ratio of 1:1. Subsequently, the micro-sized CIPs with a volume fraction of 27% were added to the mixture. Next, the mixture was well stirred in a glass cup and then was placed in a vacuum chamber for about 15 min to remove air bubbles trapped inside the material during the mixing process. Afterward, the mixture was filled into a plastic mold and was put in the vacuum chamber for about 10 min to eliminate thoroughly the air bubbles trapped inside the mixture. Finally, the mixture in the mold was cured for 24 h at room temperature (RT) in the chamber while the vacuum pump was turned off to obtain the isotropic MRE. For fabrication of anisotropic MRE, the mixture in the mold was cured for 24 h under the MFD of about 0.5 T. Microstructural morphologies of the isotropic and anisotropic MREs are described in Fig. 1. The isotropic MRE indicated randomly distributed CIPs, while the anisotropic MRE showed a chain-like structure of CIPs. The chain-like structure of CIPs created in the anisotropic MRE is attributed to the formation of the magnetic chain during the cross-linking process caused by applying the external magnetic field.

2.3 Single relaxation test and sample temperature measurement

The shear stress relaxation behavior of the isotropic and anisotropic MREs at various applied constant strains and different MFDs was investigated via the single relaxation test using double-lap shear samples. The double-lap shear samples were prepared by sandwiching two rectangular pieces of MREs ($20 \times 20 \times 5$ mm^3) between the inner and outer aluminum strips [31–33]. The single relaxation test was carried out for the isotropic and anisotropic MREs at different constant strains from 0.05 to 0.2 and the MFDs from zero to 0.58 T using an Instron Electropuls testing system with an electromagnet. The electromagnet was utilized to engender a desired external magnetic field in the perpendicular direction of the shear force. The magnetic field was applied in the parallel direction to the aligned particle chains for the anisotropic MRE. Before each relaxation test, the MRE specimen was loaded cyclically to the maximum strain to eliminate the Mullins effect. The shear force and displacement were recorded for 10 h in each single relaxation test with the crosshead speed of 5 mm/s corresponding to the strain rate of 1.0/s. The electromagnet heats the double-lap shear samples during the
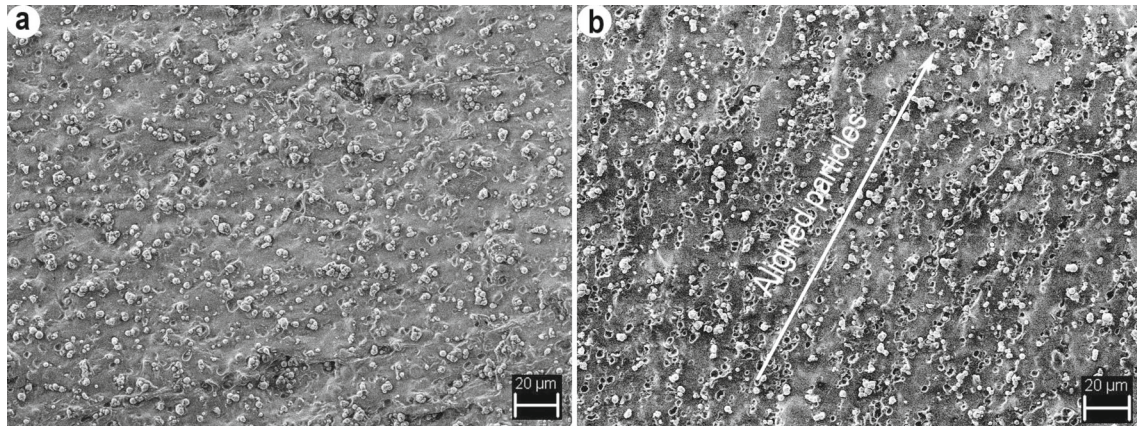
Fig. 1 SEM images showing microstructural morphologies of **a** isotropic and **b** anisotropic MREs
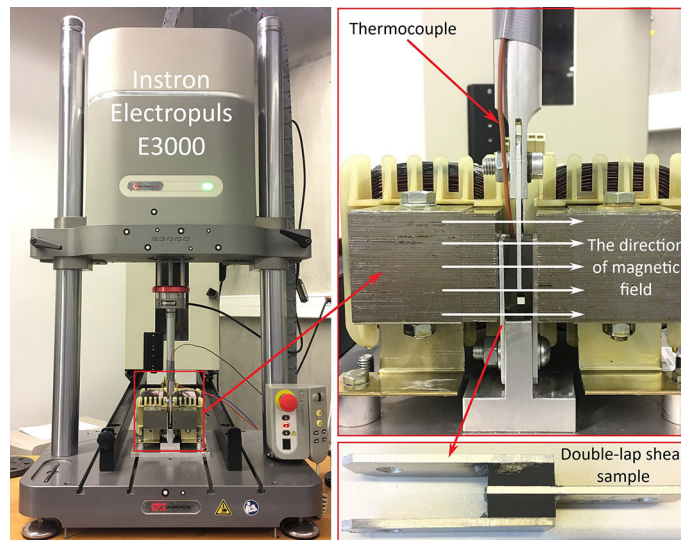

Fig. 2 The experimental setup of the shear stress relaxation test and temperature measurement on the MRE sample surface

relaxation test, resulting in the temperature rise of MRE specimens. Therefore, the measurement of the sample temperature gain is necessary to examine its effect on the shear stress relaxation of MREs. The experimental setups for the shear stress relaxation test and temperature measurement on the MRE sample surface are depicted in Fig. 2.

2.4 Results and discussion

2.4.1 The stress relaxation behavior of the MREs at different constant strains

The stress relaxation of materials under an applied constant strain is a time-dependent decrease in stress. Therefore, the applied constant strain is a significant factor influencing the stress relaxation behavior of viscoelastic materials [34]. In this study, the effects of applied constant strains on the stress relaxation response of the isotropic and anisotropic MREs in the shear mode were investigated using the single relaxation test. The shear stress and strain curves of the isotropic and anisotropic MREs at different constant strains obtained from the single relaxation test are presented in Fig. 3. The influences of applied constant strains on the shear stress of the isotropic and anisotropic MREs are described in Fig. 4. Besides, the relaxation modulus of the isotropic and anisotropic MREs at various constant strain levels is depicted in Fig. 5. The results in Fig. 3 show that the stress relaxation increases with increasing the constant strain. In addition, with the same applied
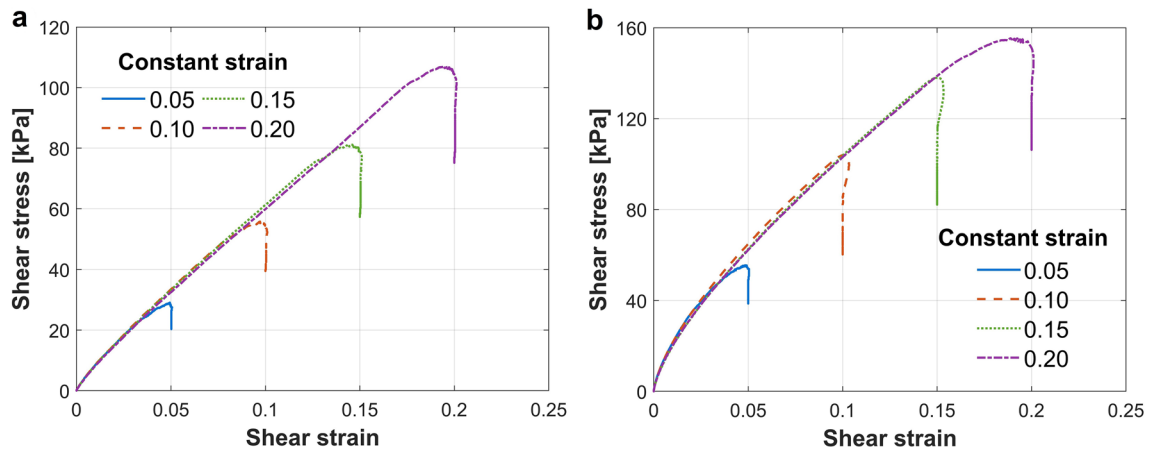
Fig. 3 Shear stress–strain curves of **a** isotropic and **b** anisotropic MREs at different constant strains
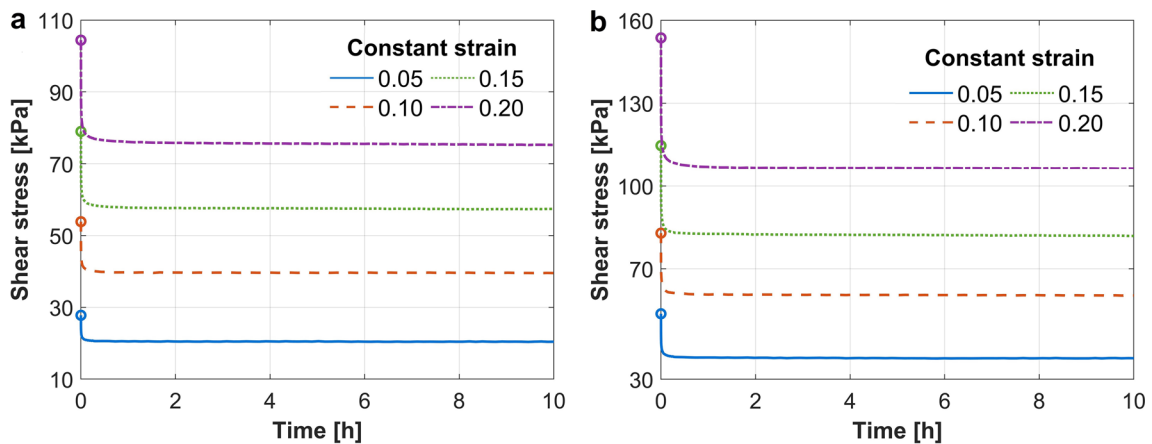

Fig. 4 Shear stress–time curves of **a** isotropic and **b** anisotropic MREs at various constant strains. The circle markers show the peak stresses

strain, the shear stress of the anisotropic MRE is much higher than that of the isotropic one. Moreover, the mechanical behavior of the isotropic MRE is different from that of the anisotropic MRE. The isotropic MRE shows linearly elastic behavior, while the anisotropic MRE has highly nonlinear elastic behavior.

The increase in the applied constant strain leads to a significant enhancement in the shear stress (Fig. 4) and a decrease in the relaxation modulus (Fig. 5). The variation of the shear stress and relaxation modulus at various constant strains can be related to process-dependent changes in the microstructure of the MREs including breakage and recovery of weak bonds of both the CIP particles and silicone matrix [32,33]. As observed in Fig. 4, the stress relaxation of the MREs enhances with the rise of the constant strain. Besides, the stress relaxation is extremely fast during the first 0.02 h, followed by a slow rate of relaxation that continues in an asymptotic sense (Fig. 4). The stress relaxation rate (SRT) is the slope of the stress relaxation curve at any point and is determined by the difference between the peak stress and current stress. The SRT of the MREs at various applied constant strains was estimated by dividing the stress difference by the time, with results presented in Table 1. As Fig. 4 and Table 1 show, the SRT of the MREs enhances with increasing the constant strain level. The SRT depends on the overstress, i.e., the difference between the current stress and the equilibrium stress [33]. The experimental results in Fig. 4 showed that the high strain level shows a larger overstress than the low strain level. The single relaxation test carried out at higher strain levels possessed greater overstresses and showed faster stress relaxation than those at lower strain levels with smaller overstresses [34].

It is observed from Fig. 4 and Table 1 that the SRT of the anisotropic MRE is higher than that of the isotropic MRE at the same constant strain. Besides, at the same applied constant strain, the shear stress and relaxation modulus of the anisotropic MRE are much greater than those of the isotropic MRE. This is explainable by the fact that the anisotropic MRE with the chain-like structure formed by aligned CIPs along
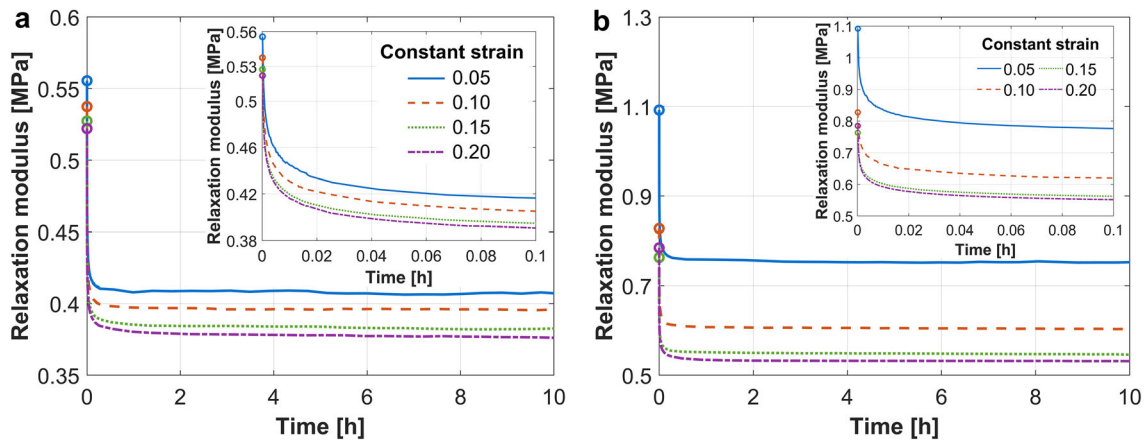
Fig. 5 Relaxation modulus curves of **a** isotropic and **b** anisotropic MREs at various constant strains. The inset is a zoom of the relaxation modulus. The circle markers show the maximal relaxation moduli

Table 1 Stress relaxation rates of isotropic and anisotropic MREs at various strains at several periods

| Time (h)	SRTs of isotropic MRE (kPa/s)				SRTs of anisotropic MRE (kPa/s)			
	0.05	0.10	0.150	0.2	0.05	0.10	0.150	0.20
0.001	0.9682	1.9202	2.9487	3.9459	2.1969	2.9761	4.4857	6.7477
0.01	0.1523	0.2986	0.4469	0.5875	0.3373	0.4674	0.6838	0.9888
0.1	0.0192	0.0368	0.0548	0.0729	0.0415	0.0584	0.0842	0.1206
0.25	0.0079	0.0153	0.0228	0.0304	0.0173	0.0241	0.0349	0.0503
0.5	0.0040	0.0078	0.0116	0.0155	0.0088	0.0122	0.0177	0.0257
1	0.0020	0.0039	0.0059	0.0079	0.0044	0.0062	0.0089	0.0130
2	0.0010	0.0020	0.0030	0.0040	0.0022	0.0031	0.0045	0.0065
5	0.0004	0.0008	0.0012	0.0016	0.0009	0.0012	0.0018	0.0026
10	0.0002	0.0004	0.0006	0.0008	0.0004	0.0006	0.0009	0.0013
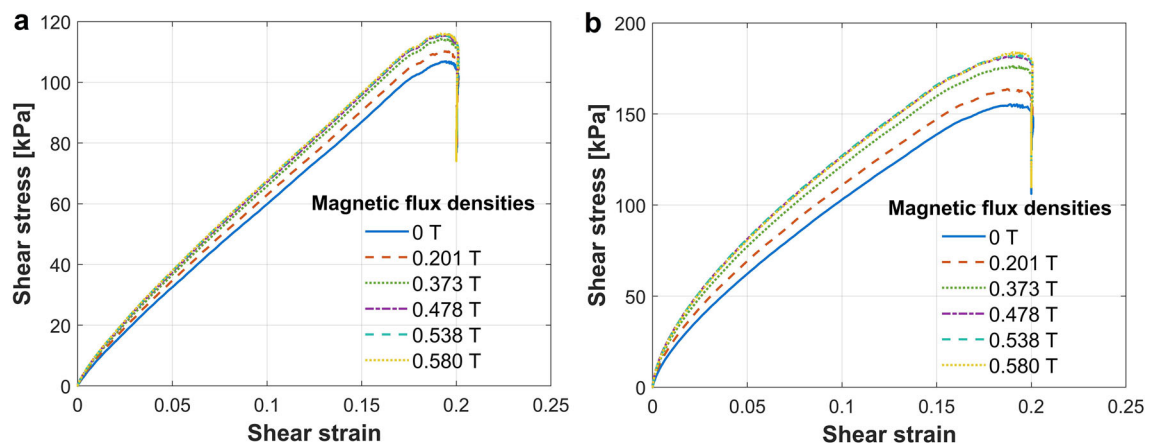
Fig. 6 Shear stress–strain curves of **a** isotropic and **b** anisotropic MREs at the constant strain of 20% under different MFDs

the magnetic field direction acts as a rod-like filler [31]. The rod-like fillers in the anisotropic MRE parallel to the applied magnetic field restrain the stretching and sliding of molecular chains of the matrix [38]. Therefore, the mechanical strength and stiffness of the anisotropic MRE are higher than those of the isotropic MRE. Moreover, the relaxation modulus of the isotropic MRE reduces slightly with increasing the constant strain from 5 to 20%, while the relaxation modulus of the anisotropic MRE considerably declines especially from 5 to 10% applied constant strain. Generally, the anisotropic MRE showed greater shear stress and relaxation modulus as well as the SRT than the isotropic MRE.
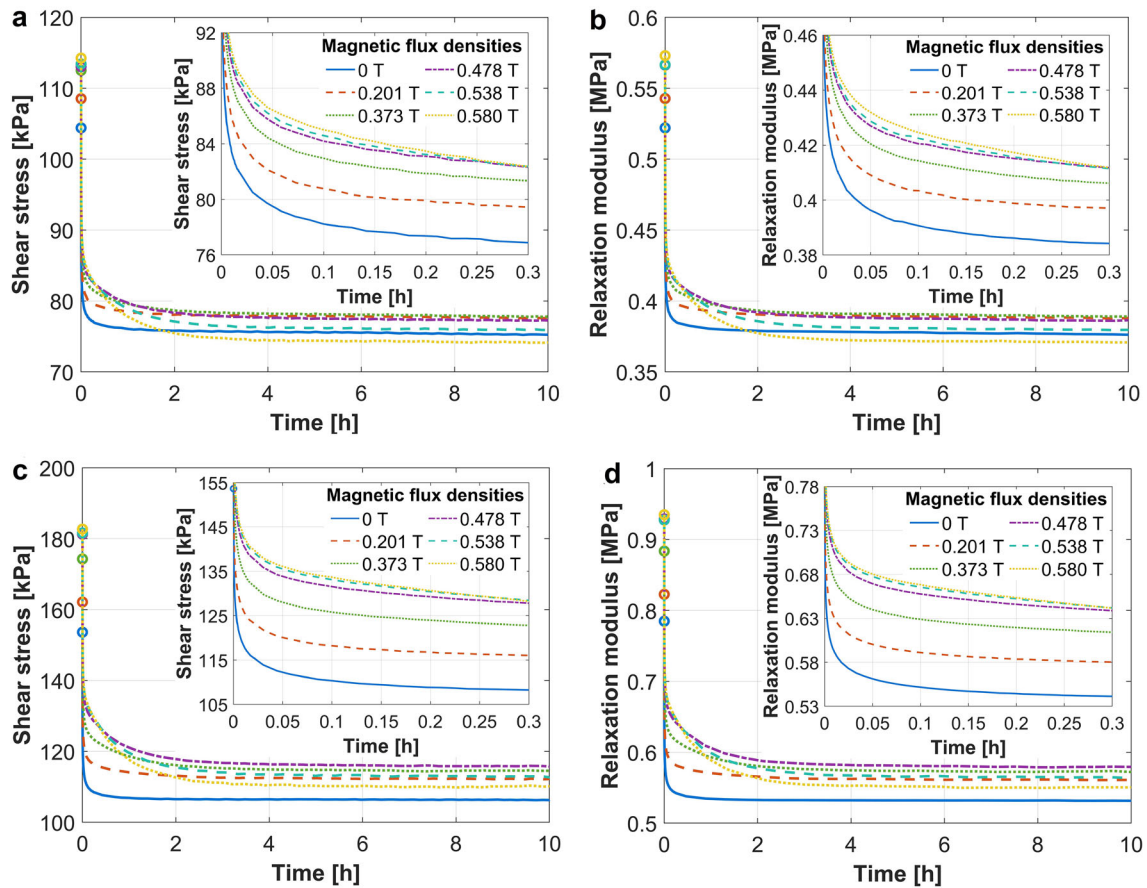
Fig. 7 Shear stress and relaxation modulus of **a**, **b** isotropic and **c**, **d** anisotropic MREs at the constant strain of 20% under different MFDs. The insets are the zooms of the shear stress and relaxation modulus. The circle markers show the peak stresses and maximal relaxation moduli

2.4.2 The stress relaxation behavior of the MREs under different MFDs

Effects of different MFDs on the stress relaxation behavior of the isotropic and anisotropic MREs at the constant strain of 20% were investigated using the single relaxation test. Figure 6 presents the shear stress–strain curves of the isotropic and anisotropic MREs at the constant strain of 20% under various MFDs. The shear stress and relaxation modulus of the isotropic and anisotropic MREs under different MFDs are described in Fig. 7. Moreover, the shear stress and modulus of the MREs in the relaxation period as a function of time and MFD are portrayed in Fig. 8. Besides, the temperature rise measured on the surface of MRE samples caused by heating of the electromagnet is depicted in Fig. 9. As described above, the shear stress–time curves indicate a strong stress relaxation at the first short period, followed by a slow relaxation rate until reaching the equilibrium state. The SRT of the isotropic and anisotropic MREs under different MFDs is given in Table 2. The SRT of the isotropic MRE is lower than that of the anisotropic MRE. It is observed from Fig. 6 that the effect of MFDs on the stress relaxation behavior of the anisotropic MRE is slightly larger than that of the isotropic one. The nonlinear behavior is visible in the case of the anisotropic MREs under different MFDs. Interestingly, the shear stress of the MREs enhances considerably with increasing the MFD to about 0.5 T, and then it changes slightly over 0.5 T. The rise is explainable that the mechanical behavior of the MREs strongly depends on the interaction level between the chains and fillers, the chains, and the fillers themselves [52].

As observed in Figs. 7 and 8, the shear stress and relaxation modulus of the isotropic MRE are lower than those of the anisotropic MRE. Besides, the shear stress and relaxation modulus of the MREs at the first 0.25 h under the MFD of 0.478 T are approximate to those under the MFD of 0.58 T. Therefore, it can be stated that the shear stress and relaxation modulus boost with the rise of the MFD to about 0.5 T for the first 0.25 h (see insets in Fig. 7). The growth in the shear stress and modulus with raising the MFD is ascribable to the
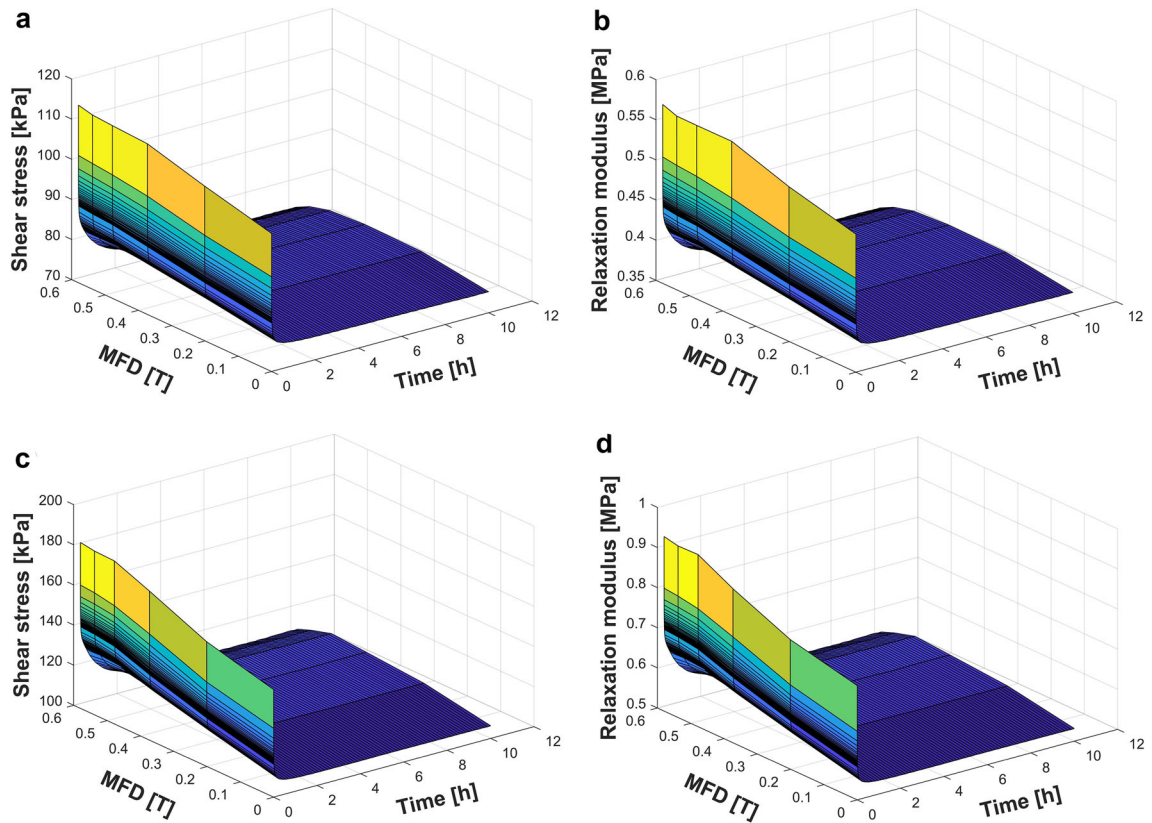
Fig. 8 Shear stress and relaxation modulus of **a**, **b** isotropic and **c**, **d** anisotropic MREs at the constant strain of 20% as functions of time and MFD
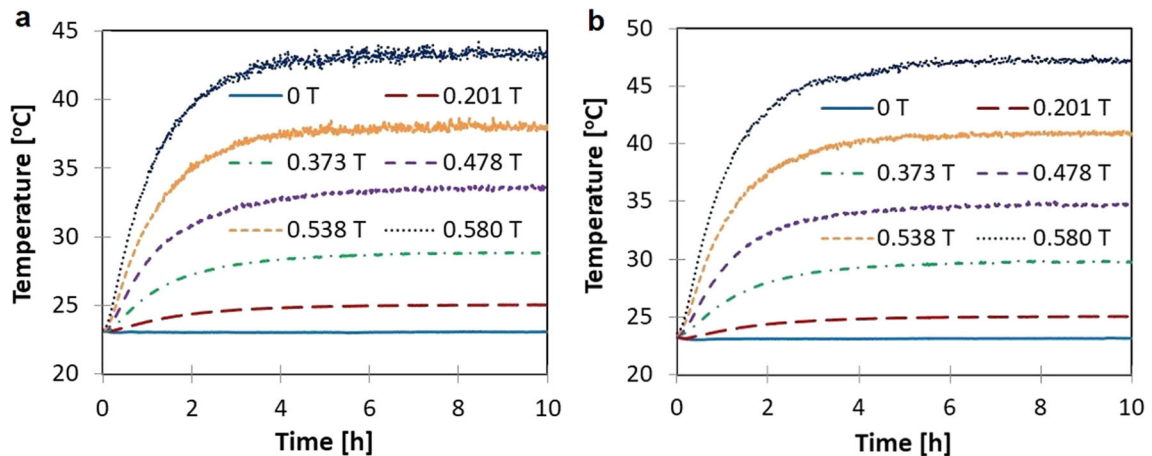

Fig. 9 Temperature rises in the isotropic **a** and anisotropic **b** MRE samples caused by heating of the electromagnet in the single relaxation test

gain of the interaction force between CIPs and silicon matrix [38]. The increase in the relaxation modulus with increasing the MFD is considered as the rise in the MR effect of the MREs [31]. Besides, the changes in the shear stress and relaxation modulus of the MREs are related to the tendency of CIPs to alter their position by applying the magnetic field. The magnetic field induces dipole moments in the ferromagnetic particles, which tend to obtain the positions of minimum energy state [32]. The movement of CIPs in the MREs under a magnetic field introduces deformations in the silicon rubber matrix, resulting in the gain of the MRE shear

Table 2 Stress relaxation rates of isotropic and anisotropic MREs under different MFDs at several periods

Time (h)	SRTs of isotropic MRE (kPa/s)					SRTs of anisotropic MRE (kPa/s)				
	0.201 T	0.373 T	0.478 T	0.538 T	0.580 T	0.201 T	0.373 T	0.478 T	0.538 T	0.580 T
0.001	4.3015	4.5051	4.3158	4.3438	4.4056	7.0088	7.6281	7.7937	7.5388	7.5007
0.01	0.6347	0.6738	0.6520	0.6521	0.6620	1.0119	1.1069	1.1289	1.0989	1.1148
0.1	0.0773	0.0825	0.0803	0.0803	0.0815	0.1224	0.1350	0.1386	0.1351	0.1368
0.25	0.0321	0.0345	0.0338	0.0341	0.0349	0.0510	0.0567	0.0588	0.0581	0.0592
0.5	0.0164	0.0177	0.0176	0.0180	0.0187	0.0261	0.0295	0.0312	0.0316	0.0327
1	0.0084	0.0092	0.0093	0.0096	0.0101	0.0133	0.0155	0.0167	0.0172	0.0181
2	0.0042	0.0047	0.0048	0.0050	0.0054	0.0068	0.0081	0.0088	0.0092	0.0097
5	0.0017	0.0019	0.0020	0.0021	0.0022	0.0028	0.0033	0.0036	0.0038	0.0040
10	0.0009	0.0010	0.0010	0.0010	0.0011	0.0014	0.0017	0.0018	0.0019	0.0020

modulus. Furthermore, the interactions between CIPs in the magnetic field bring them closer, leading to an enhancement in the stiffness of the MREs [33].

Although the shear stress and relaxation modulus of the isotropic MRE enhance with the rise of the MFD to about 0.4 T over the investigated time (Fig. 7a, b), they decrease considerably with the MFD over 0.4 T after 0.25 h. The reduction in the shear stress and relaxation modulus after 0.25 h is due to the temperature gain of the isotropic MRE sample caused by heating of the electromagnet (Fig. 9a). The electromagnet consists of wire coils wrapped around a metal core, thus it heats up when the current flows through the coils. When the MFD is lower than about 0.4 T, the maximal temperature of the isotropic MRE specimen after 0.25 h is approximately 30°C (Fig. 9a). This temperature does not affect the stress relaxation of the isotropic MRE (Fig. 7a, b). However, once the MFD is over 0.4 T, the temperature of the sample is higher than 30°C after 0.25 h and causes a decline in the shear stress and relaxation modulus of the isotropic MRE. The decrease in the shear stress and relaxation modulus of the isotropic MRE after 0.25 h increases with increasing the MFD because of the gain in the sample temperature. Besides, the sample temperature enhances rapidly at the initial period, followed by a slight rise until the stabilization (Fig. 9).

It is clear that the stress relaxation behavior of the anisotropic MRE is similar to that of the isotropic one (Figs. 7, 8). Nevertheless, the reduction in the shear stress and relaxation modulus of the anisotropic MRE after 0.25 h occurs when the MFD is over 0.48 T (Fig. 7c, d). The value of the MFD affecting the stress relaxation of the anisotropic MRE is higher than that of the isotropic MRE. This is explainable that the anisotropic MRE with the chain-like structure of CIPs is stronger than the isotropic MRE. Besides, the viscoelastic behaviors of MREs are robustly dependent on the level of interactions between the chains and fillers, the chains and the fillers themselves [32,52]. Generally, the shear stress and relaxation modulus of the MREs increase with increasing the MFD to about 0.5 T over the short time of the relaxation test. The shear stress in the relaxation period decreases with raising the sample temperature and the stress relaxes more robustly as the temperature increases. The temperature rise in the MREs causes a significant reduction in the shear stress and relaxation modulus. The decline in the relaxation stress is mainly due to easily stretching and sliding of molecular chains of the matrix under elevated temperatures [38].

3 Numerical study

3.1 Four-parameter fractional derivative model

The stress relaxation behavior of polymer materials can be examined numerically using fractional viscoelastic models [32,33,51]. Therefore, the stress relaxation behavior of the isotropic and anisotropic MREs was studied numerically using the four-parameter fractional derivative model with a one-parameter Mittag-Leffler function. The four-parameter model was composed of an elastic spring with one parameter E_0 and a fractional Maxwell element in parallel with three parameters (E_1, α, τ) [48]. The fractional derivative with the single-parameter Mittag-Leffler function is defined as [33]:

$$D^\alpha f(t) = \frac{1}{1-\alpha} \frac{\mathrm{d}}{\mathrm{d}t} \int_0^t f(x) M_\alpha \left[-\frac{\alpha(t-x)}{1-\alpha} \right] \mathrm{d}x \qquad (1)$$

where α is the fractional parameter with value changing between 0 and 1.

The one-parameter Mittag-Leffler function $M_\alpha(x)$ is defined as [52]:

$$M_\alpha(x) = \sum_{n=0}^{\infty} \frac{x^n}{\Gamma(1 + \alpha n)} \tag{2}$$

where $\Gamma(1 + \alpha n)$ is the gamma function with the argument $(1 + \alpha n)$.

The constitutive equation for the four-parameter fractional derivative model in the time domain is expressed as follows:

$$\sigma(t) + \tau^\alpha \frac{d^\alpha \sigma}{dt^\alpha} = E_0 \varepsilon(t) + (E_0 + E_1) \, \tau^\alpha \frac{d^\alpha \varepsilon}{dt^\alpha} \tag{3}$$

where E_0 and E_1 are the elastic moduli of the two springs of the model, and τ is the relaxation time of the fractional dashpot.

The relaxation modulus of the investigated model obtained by the application of the Laplace transform to Eq. (3) is expressed as follows:

$$G(t) = E_0 + E_1 M_\alpha \left[-\left(\frac{t}{\tau} \right)^\alpha \right]. \tag{4}$$

Equation (4) was used to fit the relaxation modulus of the isotropic and anisotropic MREs measured from the single relaxation test. Fitting the relaxation modulus to experimental data is finding four parameters in the vector $\mathbf{x} = (E_0, E_1, \alpha, \tau)^T$ of the fractional derivative viscoelastic model through an objective function. The objective function $f(\mathbf{x})$ is defined as the sum of squared errors [32,33].

$$f(\mathbf{x}) = \sum_{i=1}^{N} \left| G(t_i, \mathbf{x}) - G_{\exp}(t_i) \right|^2 \tag{5}$$

where N is the number of time points, and G and $G_{\exp}$, respectively, denote the predicted and measured relaxation modulus.

### 3.2 Numerical simulation of MRE stress relaxation

As presented above, the heat generation of the electromagnet during the testing influenced the stress relaxation of the isotropic and anisotropic MREs after the first 0.25 h. However, the heat generation will not occur if we use permanent magnets. In this case, the effect of temperature on the stress relaxation of the MREs will not be taken into account. Moreover, the fractional derivative model used in this study can be applied to predict the long-term stress relaxation of the MREs under different magnetic fields without the effect of heating. Therefore, the four parameters of the fractional derivative model were obtained by fitting Eq. (4) to the experimentally measured relaxation modulus for the first 0.25 h. The least-squares fit of the relaxation modulus to the measured one was conducted by minimizing the objective function with optimization options using the derivative-free method in Matlab. Effects of applied constant strains and MFDs on the stress relaxation of the MREs are numerically investigated and are presented below.

3.2.1 The MRE stress relaxation at various constant strains

The fitting model parameters to the measured data of the isotropic and anisotropic MREs at various applied constant strains are given in Table 3. The change of the parameter E_0 and fractional order α with varying the applied constant strain are presented in Fig. 10. For the isotropic MRE, the parameter E_0 changes slightly with increasing the constant strain, while the fractional order α decreases as the applied strain increase to 0.15 and then remains nearly constant (see Table 3 and Fig. 10). Unlike the isotropic MRE, the anisotropic MRE shows an insignificant change in the fractional parameter α and a reduction in E_0 with the rise of the applied constant strain. Besides, the anisotropic MRE indicates a higher elastic modulus E_0 and a lower fractional order α in comparison to the isotropic MRE. The anisotropic MRE having the chain-like particle distribution gives higher strength and modulus than those of the isotropic MRE. A smaller α indicates that the anisotropic MRE has a

Table 3 Fitting model parameters to the measured data of the isotropic and anisotropic MREs at different applied constant strains

Materials	Parameters	Applied constant strains			
		0.05	0.10	0.15	0.20
Isotropic MRE	E_0 (MPa)	0.393	0.382	0.365	0.361
	E_1 (MPa)	0.356	0.385	0.900	0.857
	α	0.348	0.332	0.284	0.279
	τ (s)	5.0E−01	2.5E−01	3.7E−03	5.4E−03
Anisotropic MRE	E_0 (MPa)	0.708	0.565	0.513	0.503
	E_1 (MPa)	4.846	1.932	1.785	7.399
	α	0.265	0.259	0.257	0.255
	τ (s)	1.0E−04	8.2E−04	8.1E−04	3.3E−06
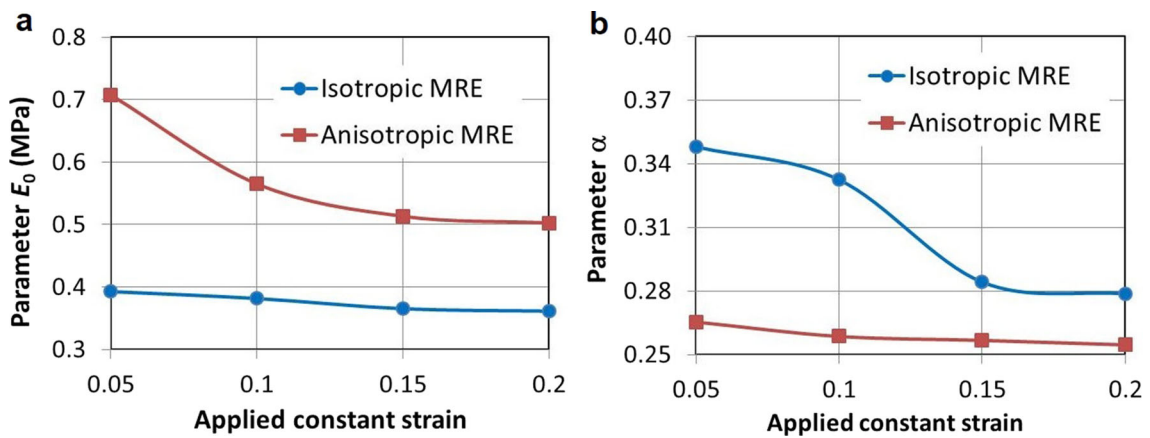
Fig. 10 The change of model parameter E_0 and fractional parameter α with varying the constant strain

broad distribution of relaxation processes [33]. This is relatable to the microstructure of the anisotropic MRE with chain-like structures of CIPs.

The measured and predicted values of relaxation modulus of the isotropic and anisotropic MREs at different applied constant strains are depicted in Fig. 11. The measured and model fitted curves of the MREs for the first 0.25 h are inserted in Fig. 11. A comparison of measured and calculated shear stress for the isotropic and anisotropic MREs is described in Fig. 12. Maximal differences between measured and model-predicted values of the shear stress and modulus for the isotropic and anisotropic MREs at various applied constant strains are given in Table 4. A very good agreement between fitted and measured relaxation modulus of the MREs is clearly observed from the insets in Fig. 11. Besides, the shear stress estimated from the investigated model for the MREs is in great agreement with the measured data for the first 0.25 h (Fig. 12). The maximal difference between measured and fitted curves for the first 0.25 h for both the relaxation modulus and shear stress is less than 1.3 % (see Table 4). It is stated that the studied model is fitted well to measured relaxation data for both isotropic and anisotropic MREs.

Moreover, although the fitting of the relaxation modulus to the measured data was performed in the first 0.25 h, the model is predictable for the stress relaxation of the MREs for a longer time. The comparisons between the measured shear stress and relaxation modulus of the isotropic and anisotropic MREs for 10 h and predicted values using the presented model are depicted in Figs. 11 and 12. As observed in Figs. 11 and 12, the calculated shear stress and relaxation modulus are in good agreement with experimentally measured ones. The maximal difference of the predicted curves for 10 h compared to the measured data for both the shear stress and relaxation modulus of the isotropic and anisotropic MREs is less than 3.7% (see Table 4). Therefore, the shear stress and relaxation modulus of the isotropic and anisotropic MREs at various applied strains can be predicted for long-term periods using the studied model with the fitted parameters. Compared with the measured shear stress at 10 h, the predicted shear stress at 1000 h reduces about 3.5% for the isotropic MRE and about 5% for the anisotropic MRE.
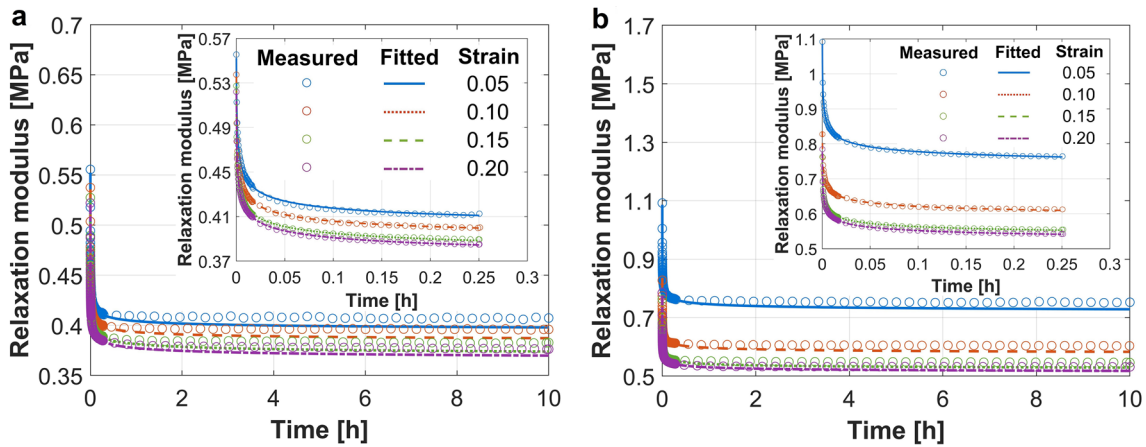
Fig. 11 Relaxation modulus (measured and predicted curves) of **a** isotropic and **b** anisotropic MREs at different constant strain levels. The insets show the model fitted curves for the first 0.25 h
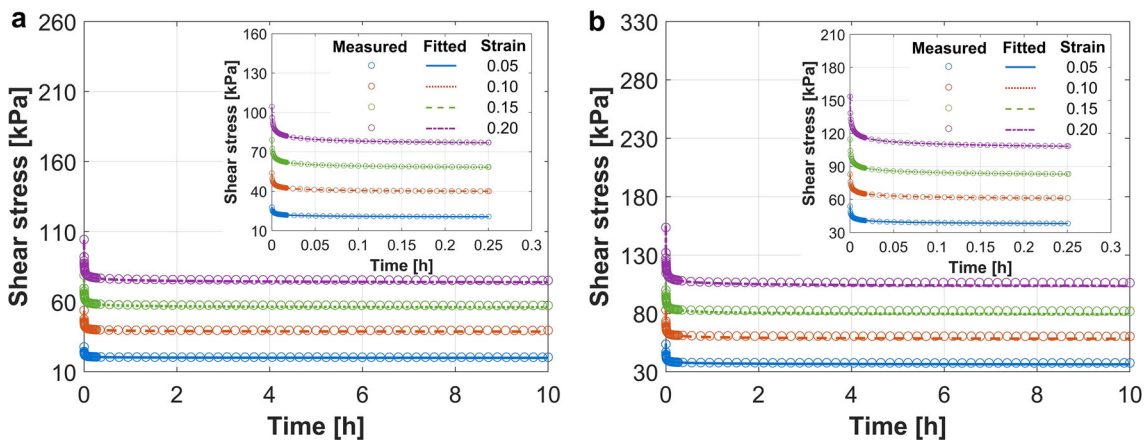

Fig. 12 Shear stress (measured and predicted curves) of **a** isotropic and **b** anisotropic MREs at different constant strain levels. The insets show the model fitted curves for the first 0.25 h

Table 4 Maximal differences between measured and model fitted values of the shear stress and modulus for the isotropic and anisotropic MREs at various applied constant strains

Materials	Time (h)	Property	Maximal differences at various applied strains (%)			
			0.05	0.10	0.15	0.20
Isotropic MRE	0.25	Modulus	0.55	0.33	0.52	0.36
		Stress	0.55	0.97	0.72	0.60
	10	Modulus	2.76	2.41	2.44	1.89
		Stress	2.76	2.41	2.44	1.89
Anisotropic MRE	0.25	Modulus	1.26	0.63	0.40	0.69
		Stress	1.26	0.63	0.40	0.74
	10	Modulus	3.54	3.65	3.45	2.72
		Stress	3.54	3.65	3.45	2.72

3.2.2 The MRE stress relaxation under various MFDs

The model fittings of the relaxation modulus with the measured data of the isotropic and anisotropic MREs under various MFDs for the first 0.25 h were conducted. Table 5 shows fitting model parameters to the measured data for the isotropic and anisotropic MREs under different MFDs. The variation of the parameter E_0 and fractional parameter α with changing the MFD is described in Fig. 13. As Table 5 and Fig. 13 show, the parameter E_0 of the isotropic and anisotropic MREs boosts with the gain of the MFD to about 0.5 T,
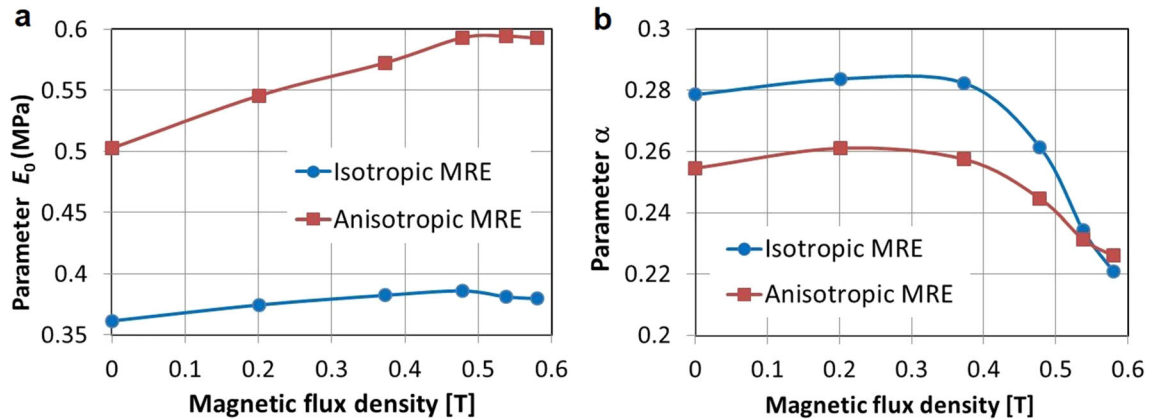
Fig. 13 The variation of model parameter E_0 and fractional parameter α with changing the MFD

Table 5 Fitting model parameters to the measured data of the isotropic and anisotropic MREs under different MFDs

| Materials	Parameters	Magnetic flux densities (T)					
		0	0.201	0.373	0.478	0.538	0.580
Isotropic MRE	E_0 (MPa)	0.361	0.374	0.382	0.386	0.381	0.380
	E_1 (MPa)	0.857	0.889	0.853	1.475	4.285	8.493
	α	0.279	0.284	0.282	0.261	0.234	0.221
	τ (s)	5.4E−03	5.4E−03	8.3E−03	5.4E−04	2.0E−06	3.8E−08
Anisotropic MRE	E_0 (MPa)	0.503	0.546	0.572	0.593	0.594	0.593
	E_1 (MPa)	7.399	9.615	13.49	8.593	13.00	20.79
	α	0.255	0.261	0.258	0.245	0.231	0.226
	τ (s)	3.3E−06	2.3E−06	4.9E−07	1.7E−06	1.2E−07	1.1E−08
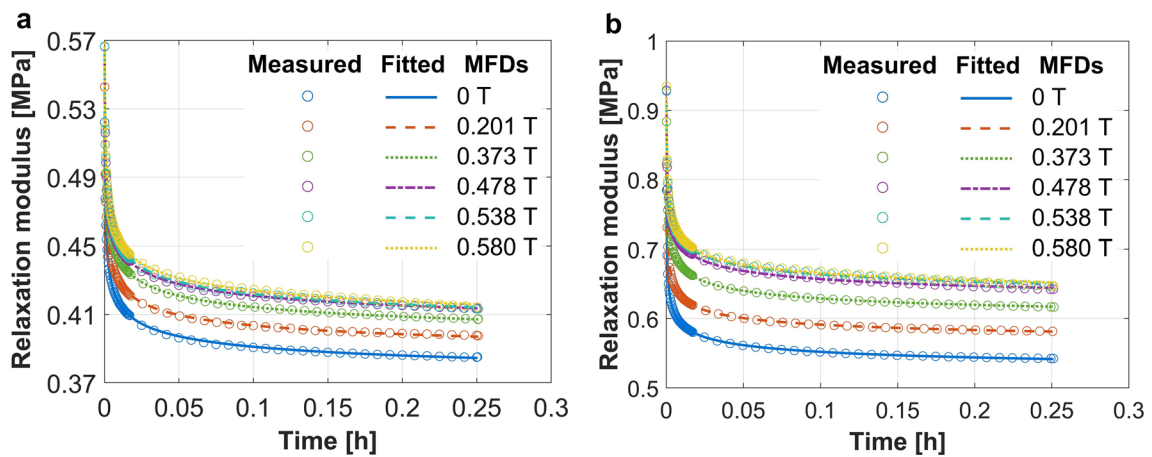
Fig. 14 Relaxation modulus (measured and model fitted curves) of **a** isotropic and **b** anisotropic MREs under different MFDs

and it changes slightly over 0.5 T. This tendency is more pronounced for the anisotropic MRE. The rise in the parameter E_0 indicated that the elastic modulus of the MREs enhances with raising the MFD, which is corresponding to the magnetic-controllable stiffness of the MREs [32,33]. Besides, the elastic modulus parameter E_0 of the anisotropic MRE is much higher than that of the isotropic MRE (Fig. 13a). It is clear from Table 5 and Fig. 13b that the fractional order α of the MREs changes slightly with increasing the MFD to about 0.4 T, and it reduces somewhat over 0.4 T. The change of fractional parameter α with varying the MFD of the isotropic MRE is similar to that of the anisotropic MRE.

The model fitted and measured values of relaxation modulus of the isotropic and anisotropic MREs under various MFDs are depicted in Fig. 14. The shear stress in the relaxation period of the isotropic and anisotropic MREs under different MFDs estimated using the investigated model with fitted parameters is presented in

Table 6 Maximal differences between measured and model fitted values of the shear stress and modulus for the isotropic and anisotropic MREs under different MFDs

| Materials	Time (h)	Property	Maximal differences under different MFDs (%)					
			0 T	0.201 T	0.373 T	0.478 T	0.538 T	0.58 T
Isotropic MRE	0.25	Modulus	0.36	0.40	0.48	0.32	0.36	0.42
		Stress	0.47	0.57	0.48	0.37	0.55	0.42
	10	Modulus	1.89	1.54	0.88	2.89	4.41	6.92
		Stress	1.89	1.54	0.88	2.89	4.41	6.92
Anisotropic MRE	0.25	Modulus	0.69	0.68	0.71	0.75	0.98	0.91
		Stress	0.74	0.99	0.95	1.02	1.28	1.21
	10	Modulus	2.72	0.68	3.42	6.10	9.21	11.68
		Stress	2.72	0.52	3.42	6.10	9.21	11.68
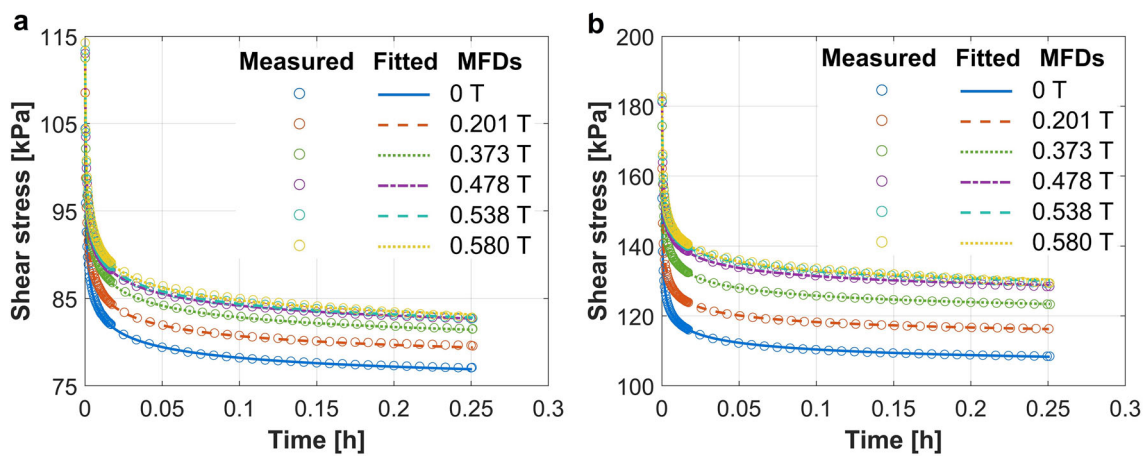
Fig. 15 Shear stress (measured and model fitted curves) of **a** isotropic and **b** anisotropic MREs under different MFDs

Fig. 15. Besides, the stress relaxation of the MREs as a function of the time under various MFDs was predicted for 10 h using the presented model with fitted parameters. A comparison between measured and predicted relaxation modulus of the isotropic and anisotropic MREs is described in Fig. 16. The measured and predicted values of the shear stress in the relaxation period of 10 h for the isotropic and anisotropic MREs under different MFDs are portrayed in Fig. 17. The maximum differences between measured and model-predicted curves of the shear stress and relaxation modulus for the isotropic and anisotropic MREs under various MFDs are given in Table 6.

A great agreement between fitted and measured relaxation modulus of the isotropic and anisotropic MREs for the first 0.25 h is clearly observed from Fig. 14. The maximum difference between the fitted and measured modulus is less than 0.5% for the isotropic MRE and 1% for the anisotropic MRE (Table 6). Besides, the shear stress estimated from the investigated model for the MREs under different MFDs is in very good agreement with the measured data (Fig. 15). Therefore, it can be stated that the four-parameter fractional derivative model is fitted well to the measured data for the MREs in the single relaxation test. However, the model prediction for 10 h relaxation is only in good agreement with the measured data of the MREs under low MFDs (Figs. 16, 17). For high MFDs, the model-predicted curves do not agree well with the experimental data of the MREs. The predicted stress and modulus of the MREs are greater than the measured ones under large MFDs. For example, under the MFD of 0.58 T, the predicted stresses of the isotropic and anisotropic MREs at 1000 h, respectively, increase approximately 4% and 9% compared to their measured stresses at 10 h. The large differences between the measured and estimated values of the shear stress and modulus of the MREs under high MFDs (Table 6) are attributed to the temperature rise in the samples caused by heating of the electromagnet. Therefore, the model fittings to the measured data of the MREs under large MFDs for a short relaxation time to predict the long-term relaxation are only acceptable if permanent magnets are used because they do not generate heat during the relaxation test. In general, the investigated model can be used to predict the long-term relaxation stress of the MREs under different magnetic fields of permanent magnets.
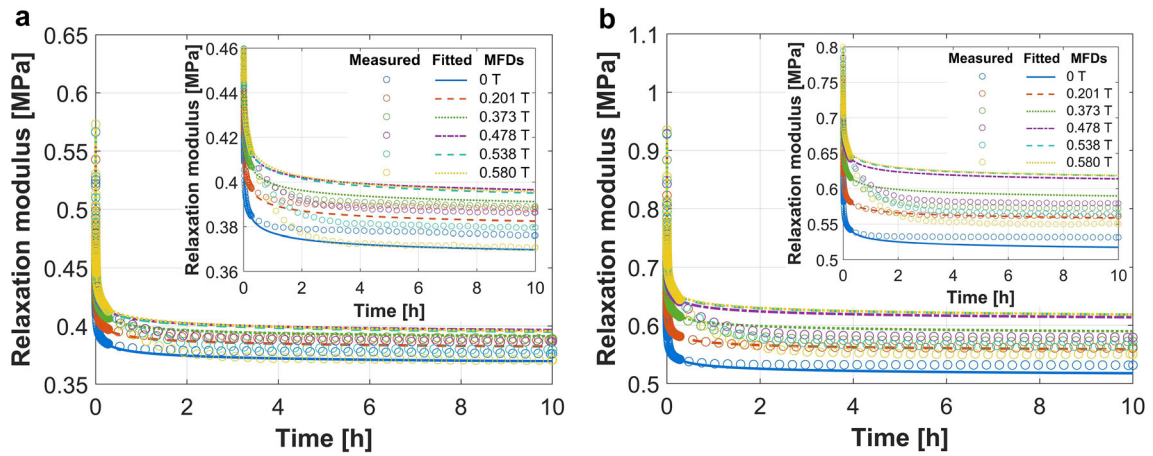
Fig. 16 Relaxation modulus (measured and model-predicted curves) of **a** isotropic and **b** anisotropic MREs under different MFDs. The inset is a zoom of the relaxation modulus
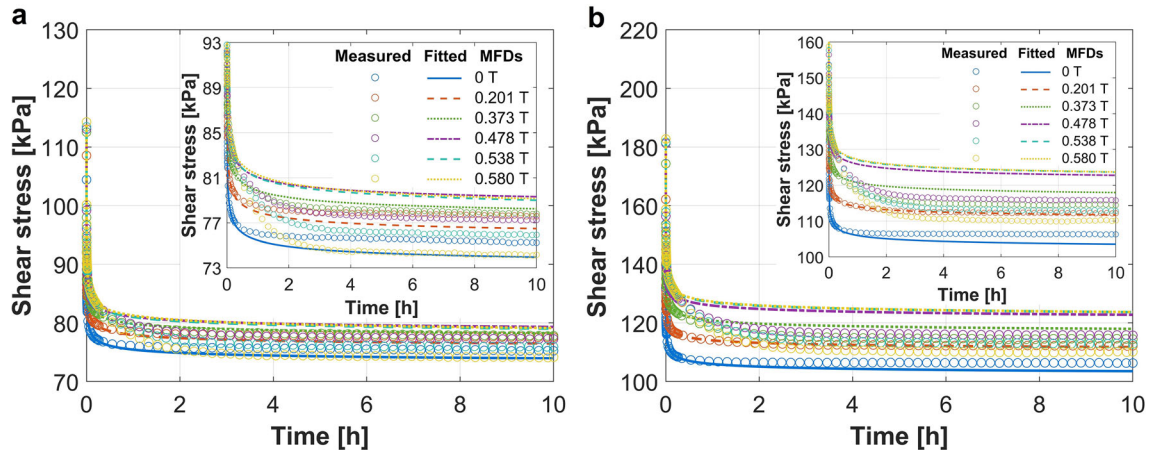

Fig. 17 Shear stress (measured and model-predicted curves) of **a** isotropic and **b** anisotropic MREs under different MFDs. The inset is a zoom of the shear stress

4 Conclusions

The experimental and numerical research of stress relaxation behavior of the isotropic and anisotropic MREs made of silicone rubber matrix and micro-sized CIPs have been conducted in this paper. Stress relaxation of the isotropic and anisotropic MREs was examined for 10 h using the single shear relaxation test. Influences of applied constant strains and magnetic fields on the stress relaxation of the MREs were studied. The isotropic MRE indicated a linearly elastic response, whereas the anisotropic MRE showed a highly nonlinear elastic behavior. The shear stress and relaxation modulus of the isotropic MRE are much lower than those of the anisotropic MRE. The shear stress of the MREs boosted with the rise of the constant strain, while the relaxation modulus decreased. The shear stress and relaxation modulus of the MREs in the first 0.25 h were enhanced with raising the MFD to about 0.5 T. After 0.25 h the shear stress and relaxation modulus of the MREs under strong magnetic fields reduced considerably because of the temperature gain in the MRE samples caused by the heat generation of the electromagnet. The stress relaxation behavior of the MREs was investigated using a four-parameter fractional derivative model. The model parameters were determined by fitting the relaxation modulus to the measured data of the MREs for the first 0.25 h. The shear stress and modulus with long-term predictions estimated from the studied model using fitted parameters were in good agreement with the measured data for the MREs at various applied strains and under low magnetic fields. The model-predicted values did not agree well with the experimental data of the MREs under high magnetic fields due to the temperature rise in the samples caused by heating of the electromagnet. Therefore, the investigated model can be used to predict the long-term relaxation stress of the MREs under high magnetic fields of permanent magnets.

Declarations

Conflict of interest The author(s) declared no potential conflicts of interest with respect to the research, authorship, and/or publication of this article.

References

1. Rigbi, Z., Jilken, L.: The response of an elastomer filled with soft ferrite to mechanical and magnetic influences. J. Magn. Magn. Mater. **37**(3), 267–276 (1983)
2. Ahamed, R., Choi, S.B., Ferdaus, M.M.: A state of art on magneto-rheological materials and their potential applications. J. Intell. Mater. Syst. Struct. **29**(10), 2051–2095 (2018)
3. Bastola, A.K., Hossain, H.: A review on magneto-mechanical characterizations of magnetorheological elastomers. Compos. B. Eng. **200**, 108348 (2020)
4. Bastola, A.K., Paudel, M., Li, L., Li, W.: Recent progress of magnetorheological elastomers: a review. Smart Mater. Struct. **29**, 123002 (2020)
5. Díez, A.G., Tubio, C.R., Etxebarria, J.G., Lanceros-Mendez, S.: Magnetorheological elastomer-based materials and devices: state of the art and future perspectives. Adv. Eng. Mater. **23**(6), 2100240 (2021)
6. Bastola, A.K., Hossain, M.: The shape-morphing performance of magnetoactive soft materials. Mater. Des. **211**, 110172 (2021)
7. Lucarini, S., Hossain, M., Garcia-Gonzalez, D.: Recent advances in hard-magnetic soft composites: synthesis, characterisation, computational modelling, and applications. Compos. Struct. **279**, 114800 (2022)
8. Deng, H.X., Gong, X.L.: Application of magnetorheological elastomer to vibration absorber. Commun. Nonlinear Sci. Numer. Simul. **13**, 1938–1947 (2008)
9. Kumbhar, S.B., Chavan, S.P., Gawade, S.S.: Adaptive tuned vibration absorber based on magnetorheological elastomer-shape memory alloy composite. Mech. Syst. Signal Process. **100**, 208–223 (2018)
10. Gao, P., Liu, H., Xiang, C., Yan, P., Mahmoud, T.: A new magnetorheological elastomer torsional vibration absorber: structural design and performance test. Mech. Sci. **12**(1), 321–332 (2021). https://doi.org/10.5194/ms-12-321-2021
11. Liao, G.J., Gong, X., Xuan, S.H., Kang, C.J., Zong, L.H.: Development of a real-time tunable stiffness and damping vibration isolator based on magnetorheological elastomer. J. Intell. Mater. Syst. Struct. **23**, 25–33 (2012)
12. Bastola, A.K., Li, L.: A new type of vibration isolator based on magnetorheological elastomer. Mater. Des. **157**, 431–436 (2018)
13. Liu, S., Feng, L., Zhao, D., Shi, X., Zhang, Y., Jiang, J., et al.: A real-time controllable electromagnetic vibration isolator based on magnetorheological elastomer with quasi-zero stiffness characteristic. Smart Mater. Struct. **28**(8), 085037 (2019)
14. Qi, S., Guo, H., Chen, J., Fu, J., Hu, C., Yu, M., Wang, Z.L.: Magnetorheological elastomers enabled high-sensitive self-powered tribo-sensor for magnetic field detection. Nanoscale **10**(10), 4745–4752 (2018)
15. Hu, T., Xuan, S., Ding, L., Gong, X.: Stretchable and magneto-sensitive strain sensor based on silver nanowire-polyurethane sponge enhanced magnetorheological elastomer. Mater. Des. **156**, 528–537 (2018)
16. Böse, H., Gerlach, T., Ehrlich, J.: Magnetorheological elastomers: an underestimated class of soft actuator materials. J. Intell. Mater. Syst. Struct. **32**(14), 1550–1564 (2021)
17. Wu, C., Zhang, Q., Fan, X., Song, Y., Zheng, Q.: Smart magnetorheological elastomer peristaltic pump. J. Intell. Mater. Syst. Struct. **30**(7), 1084–1093 (2019)
18. Lapipo, I.L., Fadly, J.D., Faris, W.F.: Characterization of magnetorheological elastomer (MRE) engine mounts. Mater. Today: Proc. **3**, 411–418 (2016)
19. Lapine, M., Shadrivov, I.V., Powell, D.A., Kivshar, Y.S.: Magnetoelastic metamaterials. Nat. Mater. **11**(1), 30–33 (2012)
20. Harne, R.L., Deng, Z., Dapino, M.J.: Adaptive magnetoelastic metamaterials: a new class of magnetorheological elastomers. J. Intell. Mater. Syst. Struct. **29**(2), 265–278 (2018)
21. Maraghechi, S., Hoefnagels, J.P.M., Peerlings, R.H.J., Rokoš, O., Geers, M.G.: Experimental full-field analysis of size effects in miniaturized cellular elastomeric metamaterials. Mater. Des. **193**, 108684 (2020)
22. Li, Y., Li, J., Tian, T., Li, W.: A highly adjustable magnetorheological elastomer base isolator for applications of real-time adaptive control. Smart Mater. Struct. **22**, 095020 (2013)
23. Testa, P., Style, R.W., Cui, J., Donnelly, C., Borisova, E., Derlet, P.M., Dufresne, E.R., Heyderman, L.J.: Magnetically addressable shape-memory and stiffening in a composite elastomer. Adv. Mater. **31**(29), 1900561 (2019)
24. Wu, S., Hu, W., Ze, Q., Sitti, M., Zhao, R.: Multifunctional magnetic soft composites: a review. Multifunct. Mater. **3**, 042003 (2020)
25. Bira, N., Dhagat, P., Davidson, J.R.: A review of magnetic elastomers and their role in soft robotics. Front. Robot. AI **7**, 146 (2020)
26. Chen, L., Gong, X.L., Jiang, W.Q., Yao, J.J., Deng, H.X., Li, W.H.: Investigation on magnetorheological elastomers based on natural rubber. J. Mater. Sci. **42**(14), 5483–5489 (2007)
27. Shit, S.C., Shah, P.: A review on silicone rubber. Natl. Acad. Sci. Lett. **36**(4), 355–365 (2013)
28. Cvek, M., Kracalik, M., Sedlacik, M., Mrlik, M., Sedlarik, V.: Reprocessing of injection molded magnetorheological elastomers based on TPE matrix. Compos. B. Eng. **172**, 253–261 (2019)
29. Li, Y., Li, J., Li, W., Du, H.: A state-of-the-art review on magnetorheological elastomer devices. Smart Mater. Struct. **23**(12), 123001 (2014)

30. Sutrisno, J., Purwanto, A., Mazlan, S.A.: Recent progress on magnetorheological solids: materials, fabrication, testing, and applications. Adv. Eng. Mater. **17**(5), 563–597 (2015)
31. Nam, T.H., Petríková, I., Marvalová, B.: Experimental characterization and viscoelastic modeling of isotropic and anisotropic magnetorheological elastomers. Polym. Test. **81**, 106272 (2020)
32. Nam, T.H., Petríková, I., Marvalová, B.: Experimental and numerical research of stress relaxation behavior of magnetorheological elastomer. Polym. Test. **93**, 106886 (2021)
33. Nam, T.H., Petríková, I., Marvalová, B.: Effects of loading rate, applied shear strain, and magnetic field on stress relaxation behavior of anisotropic magnetorheological elastomer. Mech. Adv. Mater. Struct. (2021). https://doi.org/10.1080/15376494.2021.1883162
34. Amin, A.F.M.S., Lion, A., Sekita, S., Okui, Y.: Nonlinear dependence of viscosity in modeling the rate-dependent response of natural and high damping rubbers in compression and shear: Experimental identification and numerical verification. Int. J. Plast. **22**, 1610–1657 (2006)
35. Wang, L., Han, Y.: Compressive relaxation of the stress and resistance for carbon nanotube filled silicone rubber composite. Compos. Part A Appl. Sci. Manuf. **47**, 63–71 (2013)
36. Sahu, R., Patra, K., Szpunar, J.: Experimental study and numerical modelling of creep and stress relaxation of dielectric elastomers. Strain **51**, 43–54 (2015)
37. Yamaguchi, K., Thomas, A.G., Busfield, J.J.: Stress relaxation, creep and set recovery of elastomers. Int. J. Non-Linear Mech. **68**, 66–70 (2015)
38. Qi, S., Yu, M., Fu, J., Zhu, M.: Stress relaxation behavior of magnetorheological elastomer: experimental and modeling study. J. Intell. Mater. Syst. Struct. **29**, 205–213 (2018)
39. Fan, Y., Qin, H., Lu, C., Liao, C., Chen, X., Yu, J., Xie, L.: Capacitance creep and recovery behavior of magnetorheological elastomers. J. Intell. Mater. Syst. Struct. **32**(13), 1420–1431 (2021)
40. Johari, M.A.F., Mazlan, S.A., Nordin, N.A., Aziz, S.A.A., Johari, N., Nazmi, N., Homma, K.: Shear band formation in magnetorheological elastomer under stress relaxation. Smart Mater. Struct. **30**(4), 045015 (2021)
41. Rey, T., Chagnon, G., Cam, J.B.L., Favier, D.: Influence of the temperature on the mechanical behavior of filled and unfilled silicone rubbers. Polym. Test. **32**(3), 492–501 (2013)
42. Laurent, H., Rio, G., Vandenbroucke, A., Hocine, N.A.: Experimental and numerical study on the temperature-dependent behavior of a fluoro-elastomer. Mech. Time-Depend. Mater. **18**(4), 721–742 (2014)
43. Dippel, B., Johlitz, M., Lion, A.: Thermo-mechanical couplings in elastomers-experiments and modelling. Z. Angew. Math. Mech. **95**(11), 1117–1128 (2015). https://doi.org/10.1002/zamm.201400110
44. Wan, Y., Xiong, Y., Zhang, S.: Temperature dependent dynamic mechanical properties of magnetorheological elastomers: experiment and modeling. Compos. Struct. **202**, 768–773 (2018)
45. Wen, Q., Shen, L., Li, J., Xuan, S., Li, Z., Fan, X., Li, B., Gong, X.: Temperature dependent magneto-mechanical properties of magnetorheological elastomers. J. Magn. Magn. Mater. **497**, 165998 (2020)
46. Mainardi, F.: Fractional Calculus and Waves in Linear Viscoelasticity: An Introduction to Mathematical Models. Imperial College Press, London (2010)
47. Nadzharyan, T.A., Kostrov, S.A., Stepanov, G.V., Kramarenko, E.Y.: Fractional rheological models of dynamic mechanical behavior of magnetoactive elastomers in magnetic fields. Polymer **142**, 316–329 (2018)
48. Bonfanti, A., Kaplan, J.L., Charras, G., Kabla, A.: Fractional viscoelastic models for power-law materials. Soft Matter **16**(26), 6002–6020 (2020)
49. Shen, L.J.: Fractional derivative models for viscoelastic materials at finite deformations. Int. J. Solids Struct. **190**, 226–237 (2020)
50. Su, X., Yao, D., Xu, W.: Processing of viscoelastic data via a generalized fractional model. Int. J. Eng. Sci. **161**, 103465 (2021)
51. Guo, X., Yan, G., Benyahia, L., Sahraoui, S.: Fitting stress relaxation experiments with fractional Zener model to predict high frequency moduli of polymeric acoustic foams. Mech. Time-Depend. Mater. **20**(4), 523–533 (2016)
52. Guo, Q., Zaïri, F., Guo, X.: A thermo-viscoelastic-damage constitutive model for cyclically loaded rubbers. Part II: experimental studies and parameter identification. Int. J. Plast. **101**, 58–73 (2018)